NAVAL ORDNANCE LABORATORY

(11) 29 Aug 46 (1)

(12) 15p.

(10) D. H. Rock.

[redacted]

(6)

[redacted]

[redacted] by Tulin and Burkhart, artificially [redacted] close [redacted] cavity [redacted] lutions to the problem of flow [redacted] for both models, and calculations, [redacted] numbers, N, between 0 and 1.3. Both [redacted] as [redacted] coefficient grows almost linearly [redacted] given to a close approximation by the formula [redacted] where $C_{D_0} = \frac{2\pi}{4+\pi}$ [redacted] flow on a flat plate with infinite cavity.

Foreword: The data and conclusions presented here are for the use of the personnel of the Naval Ordnance Laboratory. They may not represent the final judgment of the Laboratory.

Refs:
(a) Milne-Thompson: "Theoretical Hydrodynamics", Macmillan, Chapters 11, 12.
(b) Kreisel, G.: "Cavitation with Finite Cavitation Numbers", Admiralty Research Laboratory Report.
(c) Riabouchinski, D: "Sur les singularités des mouvements fluides", Proceedings of the Second International Congress for Applied Mechanics, pp. 512-518.

Encl:
(A) (NW) Figures 1 through 4.
(B) (NW) Tables I and II.

It is well known that ... flow of a liquid ... [illegible] ... experiments, ... [illegible] ... vapor.

[illegible] ... steady ... the static ... [illegible] ... the cavity pressure p (equal to the vapor pressure in a water tunnel), and the dynamic pressure $\frac{1}{2}\rho V^2$, where ρ = density of the liquid, V = free stream velocity. For a given ... the extent of cavitation is determined by the cavitation number,

$$K = \frac{P - p}{\frac{1}{2}\rho V^2}$$

The size of the cavity increases as K approaches zero, that is, as P approaches p or as $P/\frac{1}{2}\rho V^2$ approaches zero. In water tunnel experiments, where there are limitations on the maximum attainable velocity V, the cavitation number is reduced by letting P approach p; in water entry experiments, the dynamic head is controllable, so that $P/\frac{1}{2}\rho V^2$ can be made as small as desired.

3. The theory of the cavity formed when the static pressure in the liquid is equal to the pressure in the cavity is identical in the two-dimensional case with the theory of the infinite wake (Figure 1-a) which was first explored by Kirchhoff and Helmholtz, and later extended by Levi-Civita and others; see reference (a) for some details of this work. Physically the infinite cavity cannot occur, but can be considered as the limiting case of that occurs as the dynamic head increases without limit relative to the static pressure in the undisturbed liquid, or as the static pressure approaches the cavity pressure.

4. The Kirchhoff flow is limited to infinite cavities and zero cavitation number. An exact theory of the finite cavity corresponding to non-zero cavitation number has only recently been given. This theory is attributed to H. Wagner, although unpublished by him, and was developed independently in 1945 by G. Kreisel of the Admiralty Research Laboratory, England (reference b). The essential feature of the theory is the occurrence of a reverse jet extending from the rear of the cavity "through" the obstacle to infinity, as shown in Figure 1-b. Although this seems physically objectionable, it is a good description of what has been observed experimentally at the Naval Ordnance Laboratory. Jets do indeed occur in finite cavities, although they are either weakened by the turbulent mixing at the rear of the cavity, or finally collide with the obstacle.

[illegible] two-dimensional parallel flow [illegible] the pressure against a flat plate**. We shall assume that the free (as yet unknown) surfaces separate from the plate at the extremities of the plate and form streamlines enclosing a region of constant pressure p, (p ≤ P). The problem is to determine the flow completely, including the shape of the free streamlines. The condition can be [illegible] by Bernoulli's equation

$$\frac{1}{2}\rho V^2 + p = \frac{1}{2}\rho v^2 + P,$$

where v is the (constant) flow velocity on the free streamlines. Thus

$$\frac{v^2}{V^2} = \frac{P-p}{\frac{1}{2}\rho V^2} = 1 - \frac{1}{2}K.$$

When P = p, and therefore K = 0, the classical Kirchhoff type flow shown in Figure 1-a prevails.

8. For the case P > p, consider the flow shown in Figure 1-b. We shall need only the upper half of the flow plane, which will be designated the z-plane. The flow problem is solved once the complex velocity potential, $w(z) = \phi + i\psi$, is determined, where ϕ = velocity potential, ψ = stream function.

* This is required by the fact that the pressure always increases from the cavity into the flow.

** The following treatment can very easily be applied to wedges also.

The [illegible] on the ζ -plane are given by the [illegible]

(1) z-plane on the ζ -plane

$$\frac{dz}{d\zeta} = \frac{K_1}{(\zeta-c)[(\zeta-1)\ (\zeta-b)]^{1/2}}$$

with subsidiary conditions obtained from the known jumps in Q at 0 and c,

$$K_1 = c\sqrt{b}/2 = c\sqrt{c-1}\sqrt{c-b}$$

(A) $$\therefore \sqrt{c-1}\sqrt{c-b} = \sqrt{b}/2$$

(2) w-plane on the ζ -plane

$$\frac{dw}{d\zeta} = K_2\frac{\zeta-c}{\zeta-b}$$

with subsidiary condition

$$K_2 = \psi_0/\pi(c-b) .$$

From (1) it follows that

$$Q = \tfrac{1}{2}\log\frac{\sqrt{\zeta-b}+\sqrt{b}\sqrt{\zeta-1}}{\sqrt{\zeta-b}-\sqrt{b}\sqrt{\zeta-1}} + \log\frac{\sqrt{c-1}\sqrt{\zeta-b}+\sqrt{c-b}\sqrt{\zeta-1}}{\sqrt{c-1}\sqrt{\zeta-b}-\sqrt{c-b}\sqrt{\zeta-1}} + \log K_1 .$$

[illegible] therefore K_1 [illegible] and

[illegible]

[illegible] number. From (2) it follows that

$$\frac{\psi_0}{\pi(c-b)} \left[\zeta - (c-b)\log\left(1 - \frac{\zeta}{b}\right) \right]$$

[illegible] length l of the plate [illegible]

and

$$\frac{\psi_0}{\pi(c-b)U}\int_0^{\zeta}\left(\frac{\sqrt{\zeta-b}+\sqrt{b}\sqrt{\zeta-1}}{\sqrt{\zeta-b}-\sqrt{b}\sqrt{\zeta-1}}\right)^{\frac{1}{2}}\left(\frac{\sqrt{c-1}\sqrt{\zeta-b}+\sqrt{c-b}\sqrt{\zeta-1}}{\sqrt{c-1}\sqrt{\zeta-b}-\sqrt{c-b}\sqrt{\zeta-1}}\right)\frac{\zeta-c}{\zeta-b}\,d\zeta$$

The thickness of the jet is ψ_0/U. The shape of the cavity is given parametrically as a function of ζ ($0 \leq \zeta \leq b$) by the expression

$$\frac{1}{\pi}\frac{\psi_0}{(c-b)\,U}\int_0^{\zeta}\left(\frac{\sqrt{\zeta-b}+\sqrt{b}\sqrt{\zeta-1}}{\sqrt{\zeta-b}-\sqrt{b}\sqrt{\zeta-1}}\right)^{1/2}\left(\frac{\sqrt{c-1}\sqrt{\zeta-b}+\sqrt{c-b}\sqrt{\zeta-1}}{\sqrt{c-1}\sqrt{\zeta-b}-\sqrt{c-b}\sqrt{\zeta-1}}\right)\frac{\zeta-c}{\zeta-b}\,d\zeta$$

10. The drag is computed by integrating the excess pressure over the front face of the plate, neglecting the effect of the jet on the back face, however:

$$\text{Drag} = C_D \tfrac{1}{2}\rho l V^2 = \rho\int_0^{l/2}(U^2 - q^2)\,dy, \quad (C_D = \text{drag coefficient})$$

$$C_D = \frac{U^2}{V^2}\left(1 - \frac{\int_0^{l/2} q^2\,dy}{\frac{1}{2}\rho U^2}\right).$$

Since

$$\int_0^{l/2} q^2\,dy = -i\int_0^{l/2}\left|\frac{dw}{dz}\right|^2 dz = -i\int_0^1 \frac{\overline{dw}}{dz}\frac{dw}{d\zeta}\,d\zeta = i\int_0^1 \frac{dw}{dz}\frac{dw}{d\zeta}\,d\zeta$$

then

$$C_D = \frac{U^2}{V^2}(1 - I_1/I_2) = (1 + K)(1 - I_1/I_2)$$

where

where [illegible] is the integrand in the integral [illegible], and the path of integration in the ζ-plane encircles the singularities [illegible]. However, the path of integration is taken as the segment [illegible] of the real axis in the ζ-plane (corresponding to [illegible] in the flow plane), and the below principal value of the [illegible] of the integral, the real part of the result is the distance between stagnation points, while the imaginary part is the thickness of the jet (which corresponds to the jump at ζ_3).*

11. The integrals in the expression for C_D can be written in terms of elementary functions. C_D was evaluated for cavitation numbers between 0 and 1.5. The curve of drag coefficient vs. cavitation number is shown in Figure 2, and is seen to be almost a straight line. The variation of I_1/I_2 with cavitation number is shown in Figure 3; over the region considered the total variation remains less than 8%. To a good approximation, it follows

$$C_D = C_{D_o}(1+\sigma) \approx 0.88(1+\sigma)$$

where $C_{D_o} = 0.88$ is the drag coefficient of a flat plate with infinite cavity and zero cavitation number, the well-known result of Kirchhoff. Table I shows the variation of the different parameters and integrals.

12. Calculations of the thickness of the jet show it to be essentially constant and equal to 22% of the plate width over the considered region of cavitation numbers.

13. The length of the cavity, which is taken to be the distance between stagnation points, is plotted in units of plate width in Figure

* The preceding analysis is contained essentially in reference (b).

[illegible] cavity

[illegible] the first [illegible] [illegible] [illegible], that is, that thrust on it is equal to the force on the forward obstacle, so that the total force on the flat's cavity is zero, as would be expected from the D'Alembert paradox.

16. The calculation of the flow about two plates connected by a free boundary proceeds similarly to the previous calculation. The upper half of the z-plane (i.e. the flow plane) is taken on the w-plane as shown in Figure 4-b. Corresponding points on the two planes have the same lettering. The mapping of the boundaries of the z-planes is shown in Figure 4-c, which, as before is readily obtained from the conditions that the flow direction is constant on the two obstacles, while the flow velocity is constant on the free boundary. The mapping of the z-plane on the w-plane is here achieved directly by means of the Schwarz-Christoffel transformation

$$\frac{dQ}{dw} = \frac{K_1}{(w^2-a^2)^{1/2}(w^2-b^2)^{1/2}}$$

giving

$$Q = K_1 \cosh^{-1}\left[\frac{\frac{a}{\sqrt{a^2-b^2}} - \frac{\sqrt{w^2-b^2}+\sqrt{a^2-b^2}}{w+a}}{\frac{a}{\sqrt{a^2-b^2}} + \frac{\sqrt{w^2-b^2}+\sqrt{a^2-b^2}}{w-a}}\right]$$

The conditions

$$Q = 0 \text{ at } w = 0, \quad Q = -i\pi/2 \text{ at } w = 1$$

give $K_2 = 0$, $K_1 = -1/2$, and therefore, since $Q = \log U\frac{ds}{dw}$

- Note that the distance between the plates for a flow with preassigned cavitation number is one of the unknowns of the problems. Conversely, if the position of the plates is fixed, the cavitation number is unknown.

(b) $C_D = \frac{\quad}{\quad}$

where now

(b') $I_1 = -\int (\quad)\, dw'$

(b'') $I_2 = \int \quad dw'$

being given by (a) above. These integrals are evaluated in terms of elliptic integrals:

$$-I_1 = -E(k, \pi/2) - F(k, \pi/2) + (t^2 - \quad)$$
$$I_2 = t^2 E(k, \pi/2) - F(k, \pi/2) + (t^2 - \quad) \qquad (k = \sqrt{t^2 - 1}/t)$$

where E and F are the complete elliptic integrals of the first and second kind, respectively.

17. The length of the cavity, which is the distance between stagnation points A, A' is given by

$$-\frac{\ell}{2} \frac{\int_A^{A'} I\, dw'}{\int I\, dw'} .$$

If the upper integral is replaced by $\int_0^t I dw'$, the real part of the resulting expression represents the half-distance between stagnation

[illegible] from one another [illegible] the exact [illegible] cavitation number is known to [illegible]

[illegible] evaluation of the cavity length shows [illegible] similar agreement between the two theories. The cavity lengths and diameters are tabulated in Table II in units of the plate width, and the former is plotted as a function of cavitation number in Figure 8, where [illegible] compared with the cavity length calculated from the Wagner model. The agreement between the two theories is seen here also to be remarkable [illegible] although deviations begin to appear at high cavitation [illegible] cavitation numbers, [illegible] in the units of [illegible]

[illegible] The numerical agreement between these essentially dissimilar theories is not surprising, since the only significant physical difference between the two occurs at the rear portion of the cavity, where it would not be expected to affect the drag, cavity length, or other features of the flow in the large. The finite cavities observed in water-entry or water tunnel studies differ from the two models studied here briefly in the situation at the rear of the cavity. Turbulent [illegible] of the converging streams of liquid at the rear stagnation point results in a much weakened jet, or none at all, so that the pressure distribution are intermediate in shape between the two theoretical models. Although measurements have not been made on two-dimensional cavities to confirm the results presented here, water tunnel studies on the flow about a flat disk, in which the pressures over the face of the disk were integrated to obtain the drag, show a similar linear variation of drag coefficient. This would seem to confirm the results presented here for the corresponding two-dimensional flow.

21. Mathematical solutions do not yet exist for any three-dimensional cavity flows. The applicability of analytic methods seems to be unlikely at present. The close agreement between the simplified Riabouchinski model of the cavity and the basically correct Wagner model suggests that the former will give an accurate description of the three-dimensional cavity flow, and at the same time this model offers some

hope of successful surgical treatment. A search aimed [illegible] adequacy of [illegible] can also be obtained from already available experimental [illegible] from the [illegible] point of view, [illegible] information [illegible] [illegible] methods. [illegible]

D. GILBERT

D. H. ROCK

PLATE I

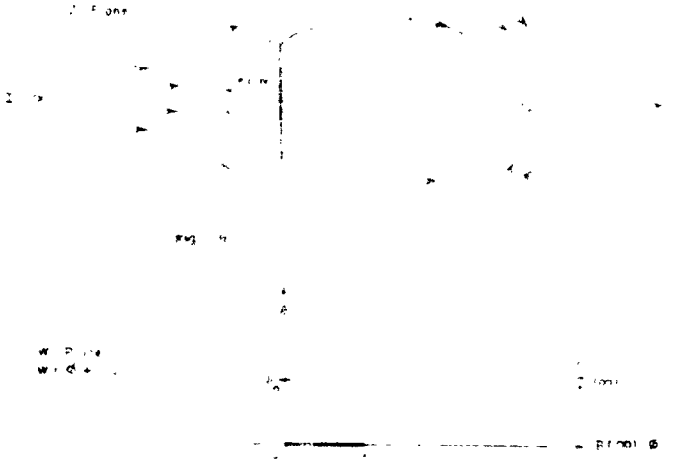

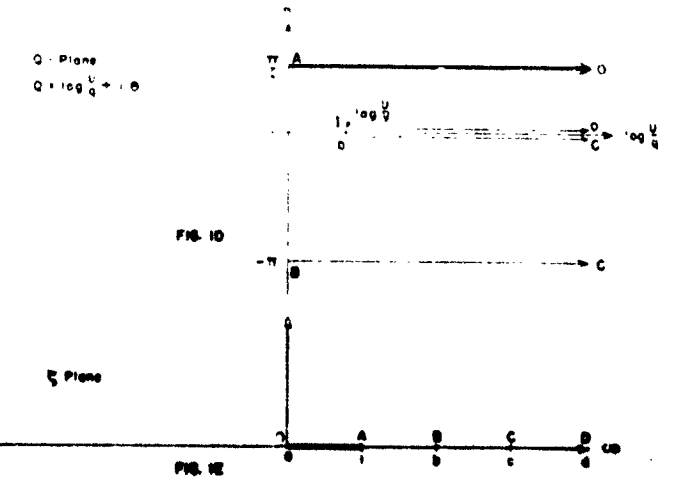

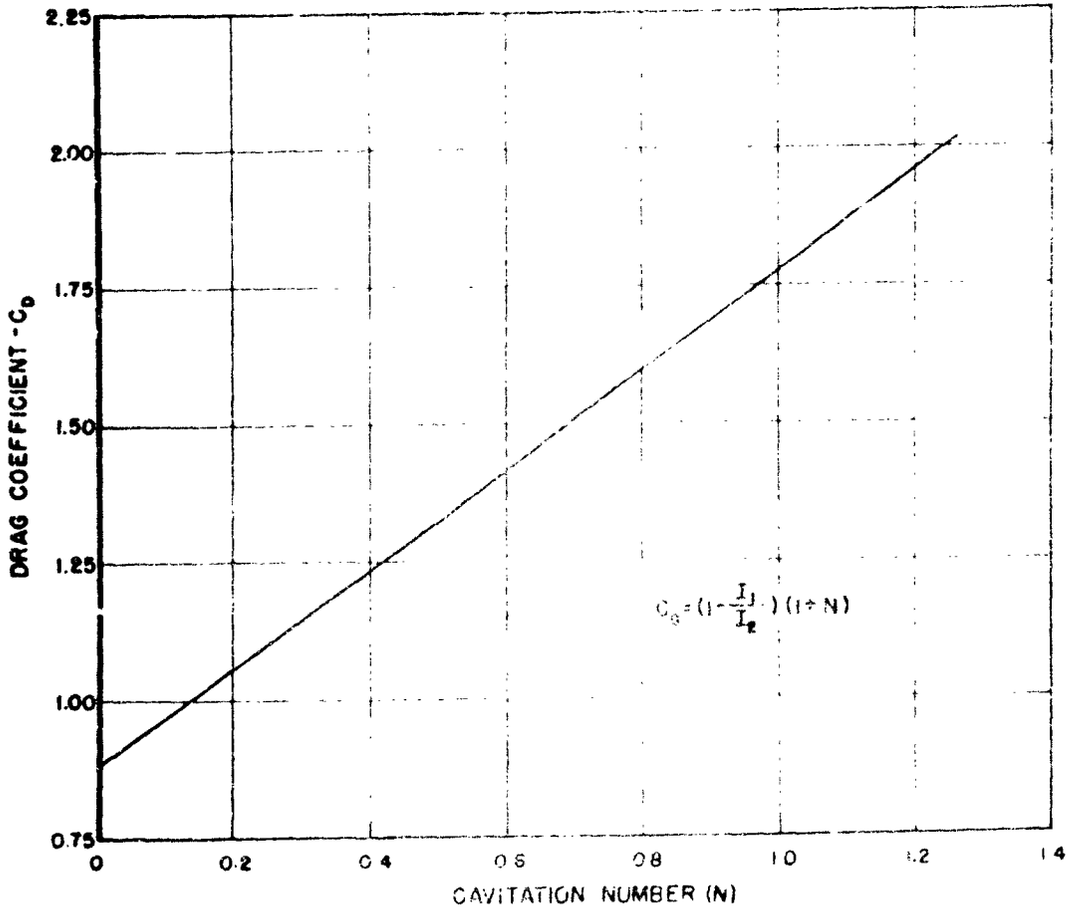

DRAG COEFFICIENT AS FUNCTION OF CAVITATION NUMBER

PLATE 2

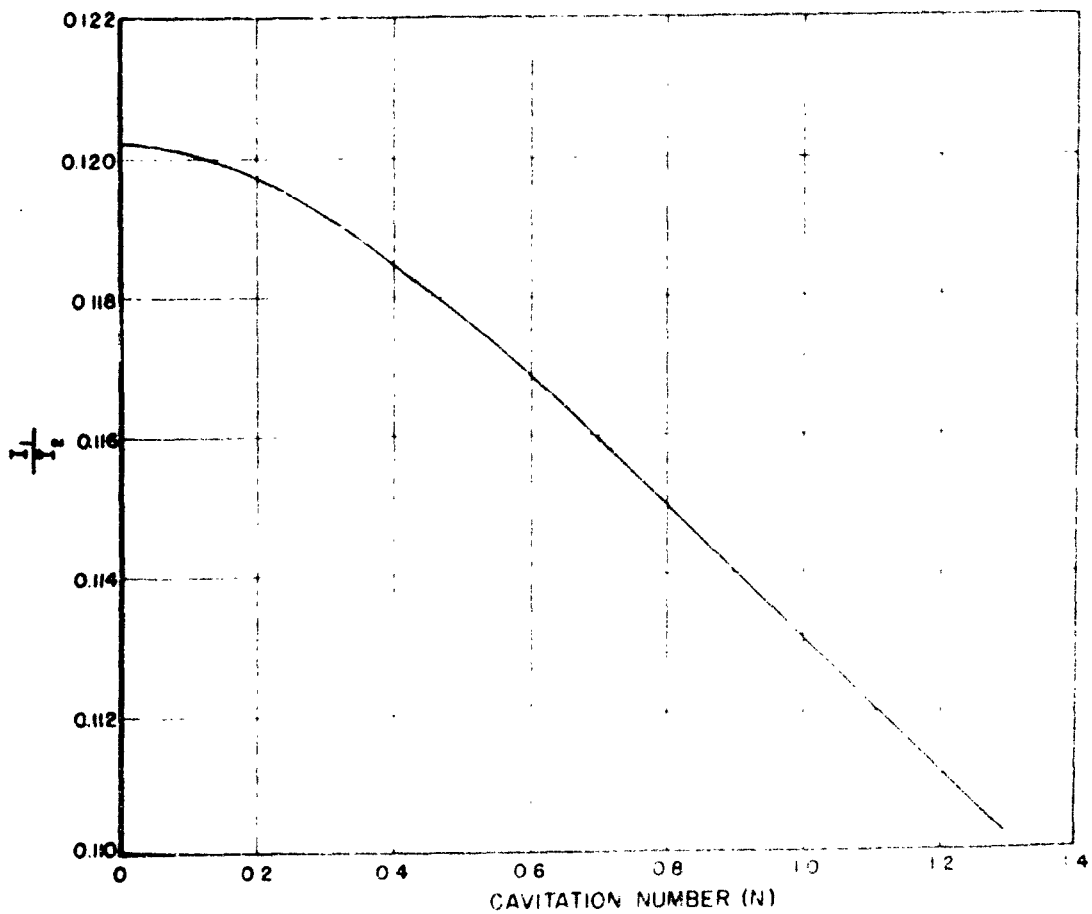

VARIATION OF I_1/I_2 WITH CAVITATION NUMBER

PLATE 5

PLATE 4

FIG 4A

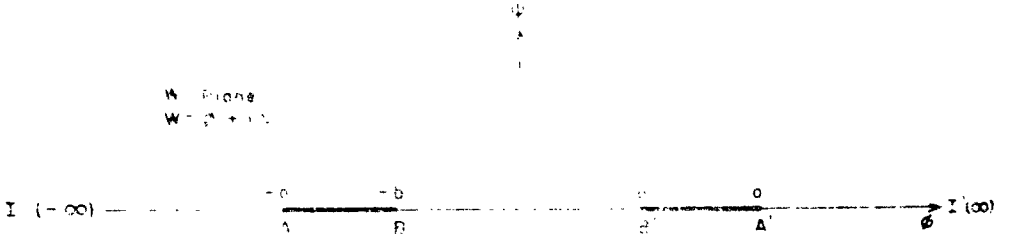

FIG 4B

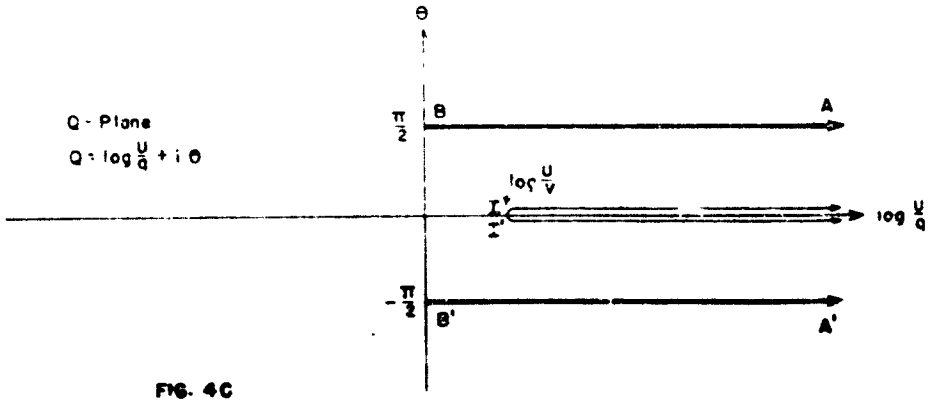

FIG. 4C

Table I

Numerical Values for [illegible] Germer Model

		0.2500					
		0.2503	0.4290				
		0.2504	0.4287	3.582			
		0.2508	0.4281	3.594	0.1191	0.2198	30.97
		0.2513	0.4275	3.608	0.1185	0.2186	19.63
		0.2519	0.4267	3.624		0.2183	
		0.2553	0.4222	3.723		0.2154	
		0.2577	0.4191	3.795		0.2133	3.198

Table II

Numerical Values for the Rimbouchinski Model

M	$i_1 x_{10^6}$	$i_2 x_{10^6}$	I_o/I_o	τ	$-i_1 x$ gravity depth	$-i_1 x$ gravity diameter
0.094	4.293	35.72	0.1202	1.001	279.1	12.97
0.196	17.14	143.2	0.1197	1.004	69.18	6.72
0.308	38.48	323.1	0.1191	1.009	30.41	4.64
0.397	59.74	504.2	0.1185	1.014	19.36	3.82
0.491	85.14	722.9	0.1178	1.020	13.41	3.28
0.604	118.8	1016.9	0.1168	1.028	9.45	2.85
0.695	148.1	1276.4	0.1160	1.035	7.48	2.61
0.794	181.9	1575.6	0.1151	1.043	6.02	2.40
0.901	218.5	1895.6	0.1141	1.052	4.98	2.24
1.004	255.4	2259.0	0.1131	1.061	4.15	2.11